

## **Physical-chemical properties of cross-linked chitosan electrospun fiber mats**

V. Sencadas<sup>1,2</sup>; D. M. Correia<sup>3</sup>; C. Ribeiro<sup>1</sup>; S. Moreira<sup>4</sup>, G. Botelho<sup>3</sup>; J. L. Gómez Ribelles<sup>5,6</sup> and S. Lanceros-Mendez<sup>1,7</sup>

<sup>1</sup> *Centro/Departamento de Física, Universidade do Minho, Campus de Gualtar, 4710-058 Braga, Portugal*

<sup>2</sup> *Escola Superior de Tecnologia, Instituto Politécnico do Cávado e do Ave, Campus do IPCA, 4750-810, Barcelos, Portugal.*

<sup>3</sup> *Dept. Química, Centro de Química, Universidade do Minho, Campus de Gualtar, 4710-057 Braga, Portugal;*

<sup>4</sup> *IBB – Institute for Biotechnology and Bioengineering, Centre of Biological Engineering, Universidade do Minho, Campus de Gualtar, 4710-057 Braga, Portugal*

<sup>5</sup> *Center for Biomaterials and Tissue Engineering, Universitat Politècnica de València, Camino de Vera s/n, 46022 Valencia, Spain*

<sup>6</sup> *Networking Research Center on Bioengineering, Biomaterials and Nanomedicine (CIBER-BBN), Valencia, Spain*

<sup>7</sup> *International Iberian Nanotechnology Laboratory - INL, Avenida Mestre José Veiga s/n 4715-330, Braga, Portugal*

\*e-mail: vsencadas@fisica.uminho.pt

## **Abstract**

Chitosan fiber mats were successfully processed by electrospinning. The as-spun fiber mats were neutralized with ethanol and cross-linked with glutaraldehyde. A decrease of the fiber average diameter from  $243 \pm 43$  nm down to 215.53 nm was observed for the neutralized and cross-linking chitosan membrane. It was found that the processing conditions do not alter the initial deacetylation degree of the polymer.

Polymer crystallinity index showed a decrease from 61 % for the Protasan material down to 17 % for the cross-linking fiber mats. A swelling index up to 1000 % was observed for the cross-linked samples. Preliminary MC-3T3-E1 cell culture results showed good cell adhesion and proliferation in the cross-linked chitosan fiber mats.

## **Introduction**

Biomaterials derived from polymers obtained from natural resources have attracted strong interest for applications in the biomedical field due to their biocompatibility and biomechanical performance. Recently, much attention has been paid to the production of nanofiber mats and scaffolds made of polymers of natural origin such as chitosan [1]. Chitosan is the deacetylated derivative of chitin, which is the second most abundant polysaccharide found in nature, after cellulose. Chitosan has several interesting properties such as biodegradability, lack of toxicity, antifungal effects, acceleration of tissue regeneration, hemostatic nature and immune system stimulation that make it an attractive material for medical applications [2-5].

The production of nanofibers by electrospinning has received increased attention due to its versatility in fiber mats production with high surface/volume ratio, high porosity and good physical, chemical and mechanical properties that can be efficiently controlled by

the variation of solution parameters and process conditions [6, 7]. Electrospinning involves the application of a high electric voltage between a conductive capillary attached to a reservoir containing a liquid polymer and a metallic collector. The strong electrostatic field produces a fiber jet that travels through the atmosphere allowing the solvent to evaporate, thus leading to the deposition of solid polymer fibers on the collector [7] with diameters ranging from several tens of nanometers to some micrometers [2, 8, 9]

Chitosan nanofibers have been successfully prepared by electrospinning chitosan solutions in trifluoroacetic acid (TFA) or in a co-solvent system of TFA and dichloromethane (DCM) [10, 11]. The as electrospun chitosan nanofibers obtained using these solvents present an important drawback due to the solubility of the nanofibers in neutral or basic aqueous solutions [6]. The dissolution of nanofibers in aqueous media occurs as a result of the high solubility of the salt side groups  $-\text{NH}_3^+$   $\text{CF}_3\text{COO}^-$  formed in the chitosan chains after the initial dissolution in TFA. A neutralization reaction then becomes a critical step after electrospinning [6].

Sangsanoh et al. [6] reported that chitosan nanofibers can be neutralized with aqueous sodium hydroxide (NaOH) and sodium carbonate ( $\text{Na}_2\text{CO}_3$ ), while Huang et al. [12] presented absolute ethanol ( $\text{CH}_3\text{CH}_2\text{OH}$ ) as a neutralizing agent of chitosan-gelatin nanofibers.

Greiner and coworkers [13] reported that nanofibers of water-soluble polymers obtained by electrospinning decompose more rapidly in contact with water, which may be favorable for some biomedical applications. However, other applications require an additional stabilization of the nanofibers, which is achieved by the crosslinking process [13], reported in the literature as the most efficient way to modify the structure of chitosan [14]. The amino group of the chitosan structure can be used in the crosslinking

process through the use of a variety of agents including diisocyanates, 1,6 (aminocarboxysulfonate) hexamethylene, genipin and glutaraldehyde (GA) [15, 16]. GA has been proposed as a crosslinking agent of the chitosan nanofibers through two main methods. One method is the Schiff base formation, in which cross-linking results in imine type functionality; the other is Michael type adducts with terminal aldehydes that lead to the formation of carbonyl groups [15, 16].

Schiffman et al. [16] demonstrated that cross-linked chitosan nanofibers can be produced using a one-step production method where the GA is added to the chitosan/TFA solution system before the electrospinning process. Cross-linked chitosan nanofibers can also be produced by two - step production methods: fiber production followed by a cross-linking process. After electrospun chitosan nanofibers are prepared, a procedure featuring 24 hours in vapor-phase GA can be performed to effectively crosslink nanofibers using Schiff base imine functionality [17].

After assessing the influence of the processing parameters that influence the electrospun chitosan fiber size and distribution [11], this work reports the effect of neutralization and cross-linking on physical properties, crystallinity, deacetylation degree and swelling index of polymer fiber mats. The suitability of the developed membranes for biomedical applications is proven by cell viability studies performed with mouse embryo fibroblast 3T3 cells.

## **Experimental**

### *Materials*

Chitosan, medical grade polymer, was purchased from Novamatrix (Protasan UP B 80/20) with 80-89 % degree of D-acetylation, according to the supplier information, and apparent viscosity of 20-199 mPa.s [18]. Dichloromethane (DCM, 99 %, Merck) and Trifluoroacetic acid (TFA, 99 %, ReagentPlus) were purchased from Sigma-Aldrich. All materials were used as received.

### *Electrospinning*

The polymer was dissolved in a TFA/DCM (70:30 % v/v) solution with 7 % weight / total solvent volume of chitosan. The solution were prepared under magnetic stirring (JPSelecta, Agimatic-E) at room temperature until complete dissolution of chitosan. The polymer solution was placed in a commercial plastic syringe fitted with a steel needle with an inner diameter of 0.5 mm. Electrospinning was conducted by applying a voltage of 25 kV with a PS/FC30P04 power source from Glassman. A syringe pump (Syringepump) fed the polymer solution into the tip at a rate of 1 ml.h<sup>-1</sup>. The electrospun samples were collected on a grounded collecting plate placed at 150 mm from the needle tip.

### *Neutralization*

As-spun chitosan fiber mats were neutralized in a vapor chamber with ethanol (99 %, Merck) for 72 h at 40 °C. After this process the samples were dried at 80 °C for another 72 h to remove the excess of ethanol.

### *Cross-linking*

Electrospun fibrous mats of chitosan were placed into a vapor chamber for 24 h under vacuum conditions. 10 mL of glutaraldehyde (GA, 50 % water, Panreac), which vaporized at room temperature, were placed at the bottom of the chamber.

### *Characterization*

Electrospun fibers were coated with a gold layer using a Polaron SC502 sputter coater and the morphology of the membranes was observed by scanning electron microscope (SEM, JSM-6300 from JEOL) at an accelerating voltage of 15 kV. The fiber diameter distribution was calculated over 50 fibers with the Image J software from the SEM images obtained at a magnification of 5000 x.

The degree of deacetylation (DD) was determined by nuclear magnetic resonance ( $^1\text{H-NMR}$ ) according to the procedure described in [19]. Five milligram of chitosan before and after the electrospinning process were added to 5 mm NMR tubes containing 0.5 mL of 2 % deuterium chloride (DCl, Fluka) solution in deuterated water ( $\text{D}_2\text{O}$ , ACROS Organics) and heated at 70 °C for 1 h. The results for the  $^1\text{H-NMR}$  were collected in a Varian Unity Plus 300 at 70 °C.

Infrared measurements (FTIR) were performed at room temperature in ABB FTLA 2000 apparatus from 4000 to 500  $\text{cm}^{-1}$ . Spectra were collected with 10 scans and a resolution of 4  $\text{cm}^{-1}$ . For the FTIR measurements, approximately 40 mg of chitosan nanofibers previously dried in a vacuum chamber for 72 h at 80 °C to constant weight, were mixed and ground with 120 mg potassium bromide. Approximately 40 mg of this mixture was put into a mold and compacted in order to obtain a disk, and then dried at 80 °C in a vacuum chamber for at least 72 hours before analysis.

X-ray patterns of the electrospun samples were performed in a X-ray diffraction instrument (Phillips Analytical X-Ray model PW 1710 BASED) with  $\text{CuK}\alpha$  monochromatic radiation at 40 kV, 30 mA and  $\lambda = 1.5406 \text{ \AA}$ , at room temperature. The relative intensity was recorded at a scattering range of  $2\theta = 4^\circ - 60^\circ$  with a step size of  $2\theta = 0.020^\circ$  and a step time of 2 s. Crystallinity index ( $C_r I_{100}$ ) was determined by the method of Focher et al. [20], using the following equation:

$$C_r I_{100} = \left[ \frac{I_{110} - I_{am}}{I_{110}} \times 100 \right] \quad \text{Eq. 1}$$

Lattice diffraction at (110),  $I_{110}$ , was measured at  $2\theta = 20^\circ$  and the amorphous region diffraction,  $I_{am}$  at  $2\theta = 16^\circ$ .

### *Swelling Behavior*

The swelling behavior was investigated using rectangular samples of  $\sim 30 \text{ mm} \times 30 \text{ mm}$  by a gravimetric method. Each sample, after submersion in phosphate buffer saline solution (PBS) (pH 7.4; 0.8 g NaCl; 0.2 g KCl; 1.44 g  $\text{Na}_2\text{HPO}_4 \cdot 2\text{H}_2\text{O}$  and 0.2 g  $\text{KH}_2\text{PO}_4$  dissolved in 1 L of distilled water) for 72 hours, was taken out and placed between two pieces of tissue paper to remove excess PBS, according to the method described elsewhere [6]. The degree of swelling (%) was calculated according to:

$$\text{Degree of Swelling}(\%) = \frac{(W_{st} - W_{dt})}{W_{dt}} \times 100 \quad \text{Eq. 2}$$

where  $W_{st}$  denotes the weight of the sample in its wet state after submersion in a PBS solution for 72 hours and  $W_{dt}$  is the weight of the sample in its dried state (72 h in a vacuum chamber at 80 °C).

### *Cell Viability Study*

For cell culture, 13 mm diameter circular chitosan membranes 13 mm were cut. For sterilization purposes, the membranes were immersed in 70 % ethanol for 30min several times. Then, the membranes were washed with phosphate-buffered saline (PBS) 5 times for 5 min to eliminate any residual ethanol.

Mouse embryo fibroblast 3T3 cells were cultivated in Dulbecco's modified Eagle's medium (DMEM) 4.5 g/L glucose (Gibco) containing 10 % newborn calf serum (Invitrogen) and 1 % of penicillin/streptomycin at 37 °C in a 95 % humidified air containing 5 % CO<sub>2</sub>.

For the study of cell viability, the 3T3 fibroblast cells were seeded in 24-well TC plates with chitosan membranes at cell density of  $3 \times 10^4$  cells/well for 2 days. For the quantification of cell viability, MTT assay (Sigma-Aldrich) was carried out. The optical density of the formazan solution was measured at 570 nm using a plate reader.

## **Results and Discussion**

### *a) Polymer morphology*

Production of reproducible and fiber size controlled chitosan fiber mats by electrospinning presents serious difficulties due to the shortage of appropriate solvents and the strong influence of processing parameters on the fiber characteristics. Chitosan



membranes were electrospun into fine, bead-free, continuous and randomly oriented fiber mats as explained in [11].

The as-spun polymer mats were subjected to a neutralization process with ethanol in a vapor chamber and under vacuum conditions for 72 h. The term “as-spun” indicates that no cross-linking or other post processing was applied to the electrospun fibers. Figure 1 show the characteristic morphology obtained for the as-spun samples (figure 1a) and for the samples with post processing chemical treatments: neutralization with ethanol (figure 1b), cross-linking with GA without previous neutralization (figure 1c) and neutralization with ethanol followed by GA cross-linking (figure 1d).

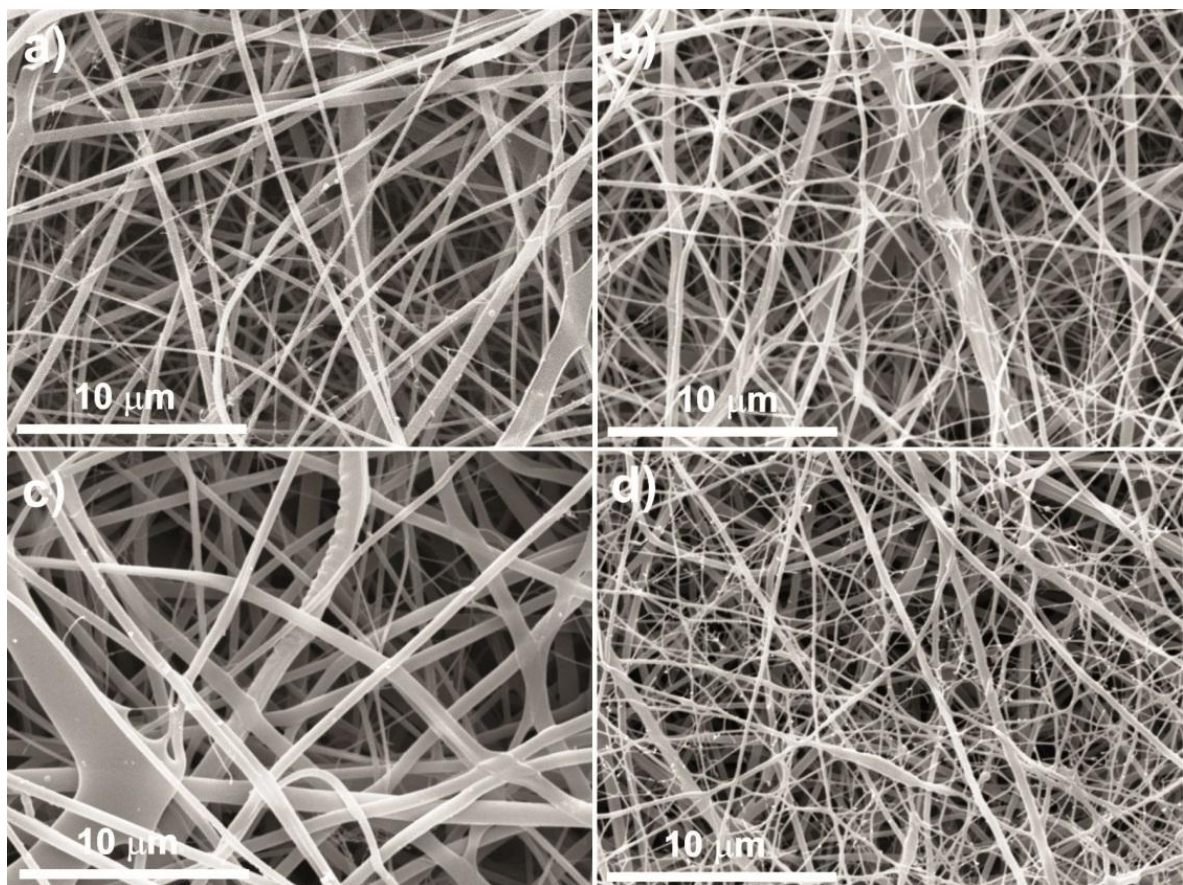


**Figure 1** – Morphology of the chitosan mats for the samples prepared from a 7 % (w/v) polymer solution, traveling distance of 15 cm, needle inner diameter of 0.5 mm, flow rate of 1 mLh<sup>-1</sup> and a voltage of 25 kV: a) as-spun fibers, b) neutralized with ethanol, c) cross-linked with GA and d) neutralized with ethanol followed by GA cross-linking.

Scanning electron microscopy showed that chitosan fiber mats after neutralization, cross-linking and neutralization followed by cross-linking retain their integrity as long randomly oriented cylindrical fibers, similar to the as-spun samples (figure 1). Fiber size distribution was obtained before and after the different chemical treatments and the results revealed that while cross-linking had no significant influence on average fiber diameter and distribution, neutralization produces a significant shrinkage of the fibers (compare figures 1a and 1b or figures 1c and 1d) with an average reduction of fiber diameter of around 10 % both in non-cross-linked and cross-linked chitosan mats (table 1).

**Table 1** – Chitosan fiber size distribution before and after neutralization, cross-linking and neutralization followed by cross-linking.

	Mean fiber diameter $\pm \sigma$ (nm)
As-spun	243 $\pm$ 43
After neutralization	219 $\pm$ 48
After cross-linking	269 $\pm$ 79
After neutralization followed by cross-linking	215 $\pm$ 53

It has been shown that the structure and dynamics of chitosan chains in solid films formed from chitosan acidic aqueous solutions strongly depend on its pH and the characteristics of the counter-ion [21]. Solutions in strong acids yield highly protonated

solid films in which residual water is strongly associated to  $-NH_3^+$  and the counter-ion, in this case trifluoroacetate. Inter and intra chain hydrogen bonding is disturbed by local interactions. When the film is neutralized by exposure to vapor ethanol, interchain hydrogen bonding between deprotonated amine  $-NH_2$  and hydroxyl groups stabilize long range ordering among chitosan chains. This process is similar to the neutralization process with  $NaOH$  (aqueous) proposed by Sangsanoh et al. [6]. Water hydration and chain reorganization is responsible for the reduction in fibril diameters shown in figure 1.

*b) Modification of the degree of deacetylation*

$^1H$ -NMR and FTIR were used to assess the chemical modifications suffered by the chitosan chains due to dissolution in TFA and further neutralization. Cross-linked samples were characterized by FTIR only since they are not soluble.

In diluted acidic media, chitosan contains glucosamine units both in protonated and neutral amine forms. For strong acid media all amine groups will be protonated whereas only a fraction of the amine groups will be protonated for weak acids such as acetic acid [21].  $^1H$ -NMR spectra did not show significant changes for the Protosan material when compared to the as-spun samples (figure 2).

The  $^1H$ -NMR spectra shown in figure 2 allow determining the DD [11, 22], that can be calculated by  $^1H$ -NMR spectroscopy using equation 3:

$$DD(\%) = \frac{H_1D}{H_1D + \frac{H_{ac}}{3}} * 100 \quad , \quad \text{Eq. 3}$$

where  $H_1D$  is the peak corresponding to the  $H_1$  proton of the deacetylated monomer (duplet at  $\delta = 4.858$  ppm) and  $H_{ac}$  is the peak of the three protons of the acetyl group (singlet at  $\delta = 1.988$  ppm) [22] The DD of commercial powder (Protasan) obtained with equation 3 was 84 %. Since Schiffman et al. [16] suggested that the electrospinning process modifies the DD of the chitosan, DD was calculated in as-spun and neutralized electrospun chitosan fiber mats, and no change with respect to original material was detected.

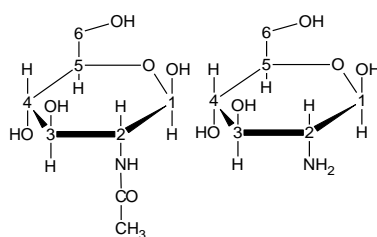


**Figure 2** - Acetylated (left) and deacetylated (right) monomers of chitosan.

Chemical characterization of the electrospun mats was completed with FTIR measurements. The obtained results for the FTIR measurements of chitosan fiber mats are shown in figure 3.

Previous studies have identified infrared absorption bands characteristic of vibrations of certain molecular groups of chitosan (table 2). In this way, the variations in the infrared spectra can be applied to monitor polymer crystallinity, water content and deacetylation degree.

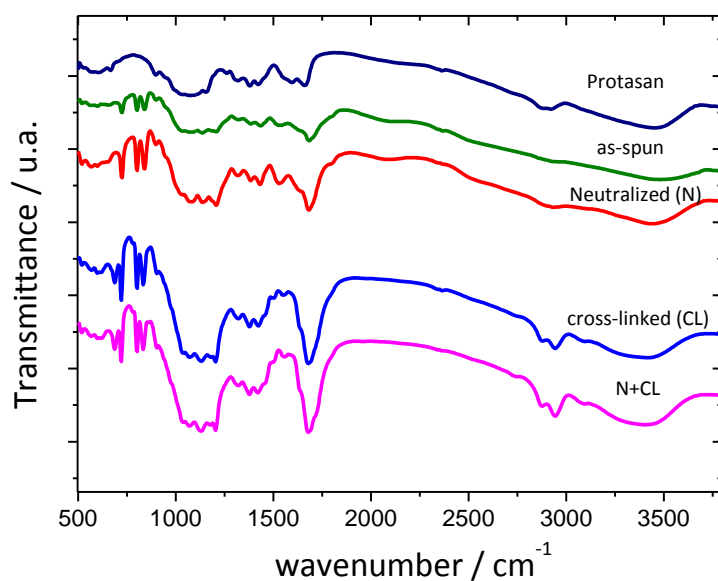


**Figure 3** - FTIR spectroscopy for the different chitosan samples.

Strong acids such TFA or HCL (hydrochloric acid) charges the polymer, inducing strong electrostatic interactions and rotational distortion around the main chain, which promotes a well-defined long range structure. Gartner et al. suggested that the large acetate counter-ion with a delocalized charge plasticizes the chitosan polymer chains enabling good long-term molecular organization, as well as increased film flexibility [21].

In figure 4, a broad absorption band between  $3500 - 3100 \text{ cm}^{-1}$  is observed corresponding to the  $-\text{OH}$  stretching mode. The aliphatic  $\text{C} - \text{H}$  stretching between  $2990$  and  $2850 \text{ cm}^{-1}$  is identified for the cross-linked and commercial samples, but for the as-spun and neutralized samples these bands are not so strong (figure 3). It is also observed that the commercial samples show a broad absorption band in this region, instead of the characteristic symmetric ( $2846 \text{ cm}^{-1}$ ) and asymmetric ( $2924 \text{ cm}^{-1}$ ) vibrational bands of  $\text{CH}_2$  (table 2).

The increase of methylene groups resulting from condensation of chitosan and GA can be followed by changes in the ratio of band intensities in the region 3000 – 2800  $\text{cm}^{-1}$ . The ratio of asymmetric and symmetric valence vibrations of  $\text{CH}_2$  groups changes due to increase of intensity of the high frequency 2924  $\text{cm}^{-1}$  absorption band, assigned to asymmetric vibrations of methylene groups at carbonyl. Together with an increase in aldehyde content groups, this suggests an elongation of the chain of intermolecular cross-links and inhomogeneity of the reaction products [15].

The absorption band corresponding to the acetylated amino group of chitin at 1647  $\text{cm}^{-1}$ , which indicates that the sample is not fully deacetylated, appears to be stronger and better defined for the neutralized and cross-linked samples followed by the cross-linking ones. Other major absorption bands between 1263 and 1088  $\text{cm}^{-1}$  represents the free primary amino group ( $-\text{NH}_2$ ) [23, 24].

As a result of cross-linking, significant changes are observed in the FTIR spectra of the cross-linked electrospun fibers when compared to the commercial and as-spun samples. A distinct change in the FTIR spectra for the carbonyl-amide region was detected. The primary amine peak decreased when the chitosan fibers were cross-linked, while a new absorption band ascribed to the  $\text{C} = \text{N}$  imine appeared at  $\sim 1650 \text{ cm}^{-1}$ , as suggested in [15, 17]. The absorption band at 1597  $\text{cm}^{-1}$  disappeared for cross-linked chitosan fiber mats due to the loss of free amines, indicating that the fibers exhibits a Schiff base imine functionality [15].

**Table 2** – Characteristic absorption bands of chitosan [24, 25].

wavenumber ( $\text{cm}^{-1}$ )	Absorption band assignment
3440	$\nu_s$ (N-H)
2924	$\nu_{as}$ (C-H)
2846	$\nu_s$ (C-H)

1647	ν (-C=O-) amide I
1597	Amine
1420, 1383	δ (C-H)
1317	ν (CH <sub>3</sub> ) amide III
1263	ν (C-O-H)
1153, 1088	ν <sub>as</sub> (C-O-C) e ν <sub>s</sub> (C-O-C)
900	ω (C-H)

Brugnerotto et al. developed a method to calculate the degree of deacetylation (DD) by FTIR for chitosan biopolymer [25]:

$$DD = 100 - \left[ \left( \frac{442.48 \cdot A_{1320}}{A_{3450}} - 13.92 \right) \right] \quad \text{Eq. 4}$$

where the  $A_{1320}$  and  $A_{3450}$  are the absorption bands at 1320 and 3450  $\text{cm}^{-1}$ , respectively. The obtained DD values for the commercial, as-spun and neutralized samples from the  $^1\text{H-NMR}$  were used as calibration for DD values obtained by FTIR. The DD value found for all samples is very similar and around 86 % ( $\pm 1\%$ ), indicating that the electrospinning, neutralization, cross-linking and neutralization followed by cross-linking processes do not change the DD value of the chitosan. Further, similar results were obtained by FTIR and  $^1\text{H-NMR}$  experiments.

The evolution of the crystallinity index for the chitosan fiber membranes after neutralization and cross-linking was evaluated by x-ray diffraction (figure 4). Chitosan can exhibit two crystalline structures, and many diffraction patterns observed by XRD typically represents mixtures of the two forms. Commercial chitosan shows two diffraction peaks, one at  $2\theta = \sim 10^\circ$  corresponding to the (010) diffraction plane of the crystalline structure I of chitosan [14, 26]. According to Julkapli et al. [14] the

orthorhombic unit cell of chitosan crystal I-form is characterized by  $a = 7.76 \text{ \AA}$ ,  $b = 10.91 \text{ \AA}$ ,  $c = 10.30 \text{ \AA}$  and  $\beta = 90^\circ$ . The diffraction peak at  $2\theta = \sim 10^\circ$  seems to be absent in as-spun sample and the sample and neutralized in ethanol, which suggests that the dissolution, electrospinning and posterior neutralization in ethanol is the origin of the chitosan crystalline structure II, corresponding to the (110) diffraction plane at  $2\theta = \sim 20^\circ$  (figure 4), but due to the broad diffraction data the presence of the  $2\theta = \sim 10^\circ$  can be hidden under the main peak. The unit cell of the chitosan form-II is characterized at  $a = 4.4 \text{ \AA}$ ,  $b = 10.0 \text{ \AA}$ ,  $c = 10.30 \text{ \AA}$  and  $\beta = 90^\circ$  [14, 26]. Moreover, for the cross-linked samples, a deviation of the (010) and (110) diffraction peaks towards lower  $2\theta^\circ$  was observed.

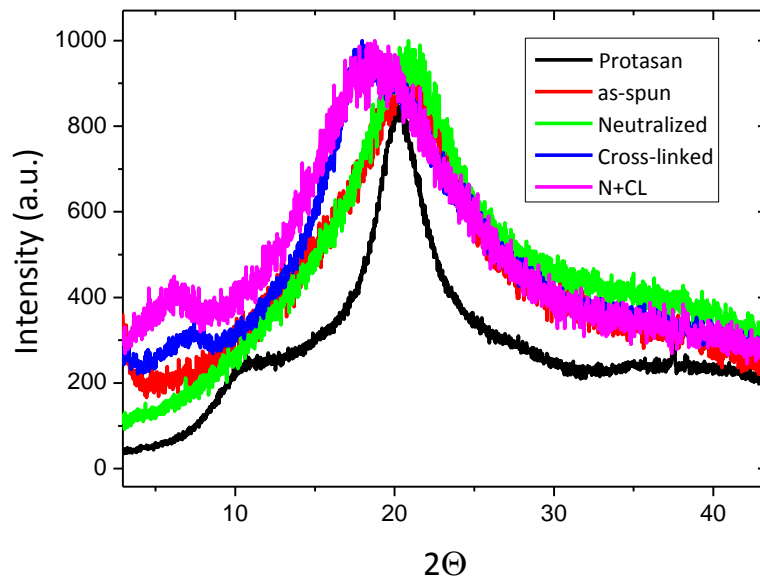


**Figure 4** - X-ray diffraction pattern for chitosan polymer.

The degree of crystallinity of chitosan decreases with the different chemical treatments applied to the membranes. The crystallinity index was calculated according to eq. 1 and the obtained results are present in table 3.



It was observed that both electrospinning and cross-linking have a strong influence on the amount of amorphous phase present in the chitosan fiber mats (Table 3). Schiffman et al. [16, 27] suggested that the electrospinning process modifies chitosan crystallinity. The comparison of the XRD spectra of as received chitosan with that of non-cross-linked electrospun mat (neutralized or not) show a quite significant changes: The observed deviation of the  $2\theta$  peak location and the decrease in crystallinity must be related with the electrospinning process. Chitosan crystallization during the electrospinning process takes place during solvent evaporation while the jet travels between the needle and the collector. While this process takes place the chitosan chains are forced in particular conformations by the strong electric fields and their diffusion to incorporate to growing crystals is compromised. Thus, it is expected not only a decrease in the total fraction of chains in the crystal phase but also a less homogeneous crystalline structure.

**Table 3** – Crystallinity index obtained for the chitosan membranes.

	$C_r I_{100}$ (%)
Protasan	61
as-spun	39
Etanol neutralized	41
Cross-linked	26
Neutralized + cross-linked	17

The effect of cross-linking is still more important. Reaction of electrospun chitosan with GA vapour induces a reorganization of polymer chains, intra and inter molecular

hydrogen bonds of chitosan network would break apart [14]. Cross-linking introduces discontinuities along the polymer chains which hinder crystal formation and the XRD peak is further shifted to lower  $2\theta$  values.

Swelling measurements are a suitable method to demonstrate the presence of crosslinking. In the case of chitosan, for a cross-linking reaction with glutaraldehyde, fewer amino groups are available on polymer backbone for protonation.

The non-cross linked samples do not swell, as they are dissolved in the PBS solution. On the other hand, the chitosan cross-linked with GA membranes and the sample neutralized and cross-linked with GA shows a swelling degree of 1000 % after 72 h in PBS solution (equation 2) which is quite high when compared to the swelling index of ~100 % found by Sangsanoh [6] or 600 % found by Li et al. [28]. Knault et al. suggests that the swelling of chitosan films is mainly influenced by ionic interactions between polymer chains, and depends on the cross-linking density achieved during the formation of the biopolymer network. In this way, increasing cross-linking density is reported to induce a decrease in the degree of swelling [17], which can also be correlated to the crystallinity decrease from 61 % (Protasan, table 3) up to 17 % for the neutralized followed by GA cross-linking polymer mats.

According to Flory [29], the degree of swelling is dependent on the cross-linking density, the affinity between the polymer and external solution, the volume of the structural unit, the fixed charge per unit of volume of the polymer, and the ionic strength of the external solution. During the chitosan cross-linking with GA, there is formation of more organized three-dimensional structure, with more free space between the polymer networks, increasing the capacity of the chitosan membrane to retain the PBS solution.

At pH around 7 the ionization of the amine groups in the chitosan network increases and the concentration of the anionic groups in the polymer network increases, resulting in an appreciable increase in the water absorbency, according to Flory theory [29].

*c) Cell culture and viability*

Electrospun chitosan membranes show a large potential for tissue and biomedical engineering applications such as wound dressing or drug delivery [30]. Some authors [31, 32] mention that GA cross-linking reveals cytotoxicity due to the unreacted aldehyde that is incorporated to the scaffold. Therefore, cell culture was performed in order to study the viability of the chitosan membranes cross-linked with GA as scaffold applications. Figure 5 shows the viability of the attached MC3T3-E1 cells on chitosan (CL and CLN) nanofibers membranes after 2 days of cell culture. Fibroblast 3T3 cell proliferation on chitosan electrospun membranes was not inhibited (figure 5). The observed trend in the two chitosan electrospun membranes is quite similar.

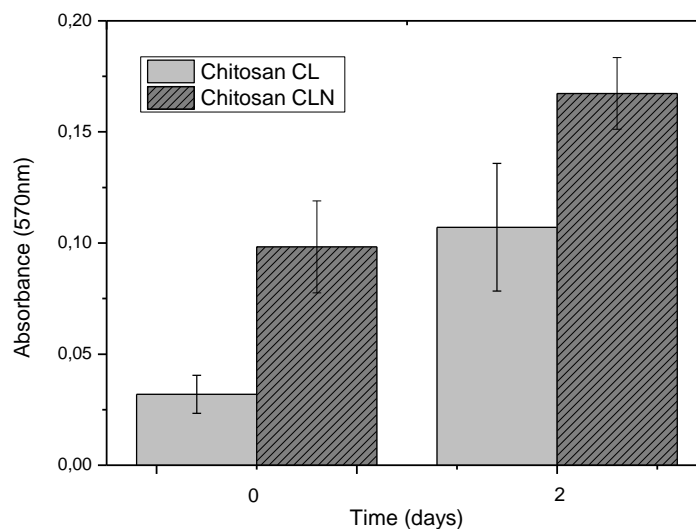


**Figure 5** - MTT absorbance results after cells seeded for 0 and 2 days on chitosan membranes: cross-linked with GA (CL) and neutralized with ethanol and subsequently cross-linked with GA (CLN). Values are mean  $\pm$  SD.

## **Conclusions**

Chitosan fiber mats were successfully processed by electrospinning. The as-spun fiber mats were neutralized with ethanol and cross-linked with GA at low pressure in a vapor chamber. A decrease of the fiber diameter from  $243 \pm 43$  down to 215.53 for the material neutralized followed by cross-linking was observed. Polymer dissolution in the TFA/DCM solvents followed by electrospinning does not change the initial degree of deacetylation of the polymer, and same result in the DD value was observed for the subsequent neutralization and cross-linking chemical treatments.

Polymer crystallinity index show a decrease from 61 % for the Protasan material down to 17 % for the sample neutralized with ethanol followed by GA cross-linking. A swelling index up to 1000 % was observed for the cross-linked samples.

The electrospinning processing and posterior neutralization and cross-linking chemical treatments does not inhibit MC-3T3-E1cell adhesion. Preliminary cell result culture results showed good cell adhesion and proliferation in the cross-linked chitosan fiber mats.

## **Acknowledgements**

This work is funded by FEDER funds through the "Programa Operacional Factores de Competitividade – COMPETE" and by national funds by FCT- Fundação para a Ciência e a Tecnologia, project references NANO/NMed-SD/0156/2007. V.S. and SM thanks the FCT grants SFRH/BPD/63148/2009 and SFRH/BPD/64726/2009, respectively. The authors also thank the support of the COST Action MP1003, 2010 'European Scientific Network for Artificial Muscles' (ESNAM). JLGR acknowledge the support of the Spanish Ministry of Science and Innovation through project No. MAT2010-21611-C03-01 (including the FEDER financial support) and Programa Nacional de Internacionalización de la I+D project EUI2008-00126. The authors also thank the National NMR Network (National Program for Scientific Re-equipment, REDE/1517/RMN/2005, funds from POCI 2010 (FEDER) and FCT) and Microscopy Service of the UPV for the use of their lab.

## **Bibliografia**

- [1] B.D. Ratner, A.S. Hoffman, F.J. Schoen, J.E. Lemons, *Biomaterials Science - An Introduction to Materials in Medicine* (2nd Edition), in, Elsevier.
- [2] X. Geng, O.-H. Kwon, J. Jang, Electrospinning of chitosan dissolved in concentrated acetic acid solution, *Biomaterials*, 26 (2005) 5427-5432.
- [3] R. Hejazi, M. Amiji, Chitosan-based gastrointestinal delivery systems, *Journal of Controlled Release*, 89 (2003) 151-165.
- [4] R.K. Majeti N.V, A review of chitin and chitosan applications, *Reactive and Functional Polymers*, 46 (2000) 1-27.
- [5] M. Dash, F. Chiellini, R.M. Ottenbrite, E. Chiellini, Chitosan—A versatile semi-synthetic polymer in biomedical applications, *Progress in Polymer Science*, 36 (2011) 981-1014.

- [6] P. Sangsanoh, P. Supaphol, Stability Improvement of Electrospun Chitosan Nanofibrous Membranes in Neutral or Weak Basic Aqueous Solutions, *Biomacromolecules*, 7 (2006) 2710-2714.
- [7] T.J. Sill, H.A. von Recum, Electrospinning: Applications in drug delivery and tissue engineering, *Biomaterials*, 29 (2008) 1989-2006.
- [8] V. Beachley, X. Wen, Polymer nanofibrous structures: Fabrication, biofunctionalization, and cell interactions, *Progress in Polymer Science*, 35 (2010) 868-892.
- [9] N. Bhardwaj, S.C. Kundu, Electrospinning: A fascinating fiber fabrication technique, *Biotechnology Advances*, 28 325-347.
- [10] K. Ohkawa, D.I. Cha, H. Kim, A. Nishida, H. Yamamoto, Electrospinning of chitosan, *Macromolecular Rapid Communications*, 25 (2004) 1600-1605.
- [11] V. Sencadas, D.M. Correia, A. Areias, G. Botelho, A.M. Fonseca, I.C. Neves, J.L. Gomez Ribelles, S. Lanceros Mendez, Determination of the parameters affecting electrospun chitosan fiber size distribution and morphology, *Carbohydrate Polymers*, 87 (2012) 1295-1301.
- [12] Y. Huang, S. Onyeri, M. Siewe, A. Moshfeghian, S.V. Madihally, In vitro characterization of chitosan-gelatin scaffolds for tissue engineering, *Biomaterials*, 26 (2005) 7616-7627.
- [13] A. Greiner, J.H. Wendorff, Electrospinning: A fascinating method for the preparation of ultrathin fibres, *Angew. Chem.-Int. Edit.*, 46 (2007) 5670-5703.
- [14] N.M. Julkapli, Z. Ahmad, H.M. Akil, X-Ray Diffraction Studies of Cross Linked Chitosan With Different Cross Linking Agents For Waste Water Treatment Application, in: A. Saat, A. H., J.M.H. H., S.J. M., O.M. R., I. A., F.M.A.M. Idris (Eds.) *Neutron and X-Ray Scattering Advancing Materials Research*, 2009, pp. 106-111.
- [15] N. Kildeeva, P. Perminov, L. Vladimirov, V. Novikov, S. Mikhailov, About mechanism of chitosan cross-linking with glutaraldehyde, *Russian Journal of Bioorganic Chemistry*, 35 (2009) 360-369.
- [16] J.D. Schiffman, C.L. Schauer, Cross-Linking Chitosan Nanofibers, *Biomacromolecules*, 8 (2006) 594-601.
- [17] J.Z. Knaul, S.M. Hudson, K.A.M. Creber, Crosslinking of chitosan fibers with dialdehydes: Proposal of a new reaction mechanism, *Journal of Polymer Science Part B: Polymer Physics*, 37 (1999) 1079-1094.
- [18] Novamatrix, Protasan - Chitosan Biopolymer, in: *Novamatrix* (Ed.), 2011.

- [19] E. Fernandez-Megia, R. Novoa-Carballal, E. Quiñoá, R. Riguera, Optimal routine conditions for the determination of the degree of acetylation of chitosan by <sup>1</sup>H-NMR, *Carbohydrate Polymers*, 61 (2005) 155-161.
- [20] B. Focher, P.L. Beltrame, A. Naggi, G. Torri, Alkaline N-deacetylation of chitin enhanced by flash treatments. Reaction kinetics and structure modifications, *Carbohydrate Polymers*, 12 (1990) 405-418.
- [21] C.a. Gartner, B.L. López, L. Sierra, R. Graf, H.W. Spiess, M. Gaborieau, Interplay between Structure and Dynamics in Chitosan Films Investigated with Solid-State NMR, Dynamic Mechanical Analysis, and X-ray Diffraction, *Biomacromolecules*, 12 (2011) 1380-1386.
- [22] M. Lavertu, Z. Xia, A.N. Serreqi, M. Berrada, A. Rodrigues, D. Wang, M.D. Buschmann, A. Gupta, A validated <sup>1</sup>H NMR method for the determination of the degree of deacetylation of chitosan, *Journal of Pharmaceutical and Biomedical Analysis*, 32 (2003) 1149-1158.
- [23] Q. Yuan, J. Shah, S. Hein, R.D.K. Misra, Controlled and extended drug release behavior of chitosan-based nanoparticle carrier, *Acta Biomaterialia*, 6 (2010) 1140-1148.
- [24] M. Huo, Y. Zhang, J. Zhou, A. Zou, D. Yu, Y. Wu, J. Li, H. Li, Synthesis and characterization of low-toxic amphiphilic chitosan derivatives and their application as micelle carrier for antitumor drug, *International Journal of Pharmaceutics*, 394 (2010) 162-173.
- [25] J. Brugnerotto, J. Lizardi, F.M. Goycoolea, W. Argüelles-Monal, J. Desbrières, M. Rinaudo, An infrared investigation in relation with chitin and chitosan characterization, *Polymer*, 42 (2001) 3569-3580.
- [26] B.W.S. Souza, M.A. Cerqueira, J.T. Martins, A. Casariego, J.A. Teixeira, A.A. Vicente, Influence of electric fields on the structure of chitosan edible coatings, *Food Hydrocolloids*, 24 (2010) 330-335.
- [27] J.D. Schiffman, L.A. Stulga, C.L. Schauer, Chitin and chitosan: Transformations due to the electrospinning process, *Polymer Engineering & Science*, 49 (2009) 1918-1928.
- [28] M. Li, B. Han, W. Liu, Preparation and properties of a drug release membrane of mitomycin C with &lt;i>N</i>-succinyl-hydroxyethyl chitosan, *Journal of Materials Science: Materials in Medicine*, 22 (2011) 2745-2755.

- [29] P.J. Flory, Principles of Polymer Chemistry, Cornell University Press, Ithaca; New York, 1953.
- [30] K. Sun, Z.H. Li, Preparations, properties and applications of chitosan based nanofibers fabricated by electrospinning, Express Polymer Letters, 5 (2011) 342-361.
- [31] B. Carreño-Gómez, R. Duncan, Evaluation of the biological properties of soluble chitosan and chitosan microspheres, International Journal of Pharmaceutics, 148 (1997) 231-240.
- [32] B. Hoffmann, D. Seitz, A. Mencke, A. Kokott, G. Ziegler, Glutaraldehyde and oxidised dextran as crosslinker reagents for chitosan-based scaffolds for cartilage tissue engineering, Journal of Materials Science: Materials in Medicine, 20 (2009) 1495-1503.